

LABORATORY AND FIELD PERFORMANCE OF MEGAPIXEL QWIP FOCAL PLANE ARRAYS

Arnold Goldberg

EO/Photonics Division, U. S. Army Research Laboratory, Adelphi, MD 20783, USA

Introduction

The quantum well infrared (IR) photodetector (QWIP) was first demonstrated nearly 20 years ago.¹ Two-dimensional staring focal plane arrays of QWIPs were developed relatively soon after this. Unlike HgCdTe, the principal competitive technology for detection in the long wavelength IR (or LWIR), the main limitation to the production of large format FPAs for QWIPs has been the availability of large format readout integrated circuits (ROICs). At the time that QWIPs were first being exploited, the largest ROIC format available was 128×128 pixels used by manufacturers of medium wavelength IR (MWIR) detector arrays using InSb. In contrast, LWIR HgCdTe has presented major detector material challenges in terms of compositional uniformity and defect density that have kept yields low and costs high. Since QWIPs are made from the relatively mature GaAs/AlGaAs material system for which a large infrastructure exists, it is a straightforward task to design, grow, and fabricate QWIP FPAs using molecular beam epitaxy (MBE) and standard process tools on GaAs substrates as large as 6 inches (15.24 cm) in diameter. An FPA with a format of 1024×1024 pixels with a pixel pitch of $20 \mu\text{m}$ will be approximately 20.5 cm long on each side. On a 6 in substrate, it is possible to process at least 16 FPAs of this size. However, the ZnCdTe substrates necessary for high-quality HgCdTe FPAs are limited to a diameter of approximately 1 in. It is impossible to process more than one 1024×1024 FPA on each substrate. As a result, the production yield for 1024×1024 LWIR FPAs using HgCdTe will be quite low until either ZnCdTe becomes available in significantly larger sizes or it is possible to grow HgCdTe on Si wafers. Much progress has been made in growing MWIR HgCdTe on Si but growth of LWIR layers on Si remains a significant challenge. Therefore, QWIP technology may be the only choice for affordable high-performance FPAs in large formats.

As the U. S. Army undergoes the transformation to the Future Force, there will be much effort put in to the development of a third generation forward looking infrared (FLIR) imaging system to replace current 2nd generation FLIRs for reconnaissance, surveillance, target acquisition, and fire control on the future combat system (FCS) vehicles. The system is envisioned to be a quantum leap in performance over present 2nd generation FLIR. To achieve this, it is envisioned that the IR FPA will need to be a large format staring sensor with more than 1000 pixels on a side. In addition, the 3rd

generation FLIR is envisioned to have a multispectral imaging capability along with advanced image processing functionality. These attributes of 3rd generation FLIR will present many challenges to the IR FPA manufacturing community. The first multispectral IR FPA with more than 1000 pixels on a side has yet to be produced. Since initial deployment of FCS will be during the present decade, much work needs to be done to make large format multispectral IR imaging a reality.

Over the last few years, there has been much effort put into the development of focal plane arrays (FPAs) capable of imaging in two bands of the IR spectrum simultaneously. Some of the motivations for dual-band IR imaging are enhanced detection of targets in clutter, the ability to distinguish between targets and decoys, and remote absolute temperature measurement. These efforts have produced IR FPAs operating at two wavelengths in the MWIR² and the LWIR³ as well as FPAs operating in both the LWIR and MWIR.⁴ It is postulated that a dual-band IR imager would be advantageous over single-color IR cameras (either LWIR or MWIR) because it could operate in a wider range of ambient conditions and be more effective in defeating IR countermeasures such as smoke, camouflage, and flares.

For almost a decade the U. S. Army Research Laboratory (ARL) has supported the development of multispectral IR imaging through the Federated Laboratory Advanced Sensors Consortium⁵ and, more recently, through the Advanced Sensors Collaborative Technology Alliance (CTA). As a result of these programs, ARL and its industry partners have produced dual-band MWIR/LWIR pixel-registered and simultaneously integrating FPAs in both the QWIP and HgCdTe based photodiode detector technologies.⁶ However, both of these FPAs are medium sized format. The MCT FPA is a 320×240 array of $50 \mu\text{m}$ pixels and the QWIP FPA is a 256×256 array of $40 \mu\text{m}$ pixels. A 3rd generation FLIR is envisioned to be of a format of roughly 1200×800 with pixel size of less than $20 \mu\text{m}$. In this paper, we will discuss recent application of QWIP technology to the production of very large format FPAs. We show the results of laboratory tests and field imagery on a single-color LWIR 1024×1024 pixel QWIP FPA.

Large Format LWIR FPAs -Motivation

Figure 1 shows imagery of people at a range of 500m taken with IR cameras with similar optics but with

Report Documentation Page

*Form Approved
OMB No. 0704-0188*

Public reporting burden for the collection of information is estimated to average 1 hour per response, including the time for reviewing instructions, searching existing data sources, gathering and maintaining the data needed, and completing and reviewing the collection of information. Send comments regarding this burden estimate or any other aspect of this collection of information, including suggestions for reducing this burden, to Washington Headquarters Services, Directorate for Information Operations and Reports, 1215 Jefferson Davis Highway, Suite 1204, Arlington VA 22202-4302. Respondents should be aware that notwithstanding any other provision of law, no person shall be subject to a penalty for failing to comply with a collection of information if it does not display a currently valid OMB control number.

1. REPORT DATE 00 DEC 2004	2. REPORT TYPE N/A	3. DATES COVERED -	
4. TITLE AND SUBTITLE Laboratory And Field Performance Of Megapixel Qwip Focal Plane Arrays		5a. CONTRACT NUMBER	
		5b. GRANT NUMBER	
		5c. PROGRAM ELEMENT NUMBER	
6. AUTHOR(S)		5d. PROJECT NUMBER	
		5e. TASK NUMBER	
		5f. WORK UNIT NUMBER	
7. PERFORMING ORGANIZATION NAME(S) AND ADDRESS(ES) EO/Photonics Division, U. S. Army Research Laboratory, Adelphi, MD 20783, USA		8. PERFORMING ORGANIZATION REPORT NUMBER	
9. SPONSORING/MONITORING AGENCY NAME(S) AND ADDRESS(ES)		10. SPONSOR/MONITOR'S ACRONYM(S)	
		11. SPONSOR/MONITOR'S REPORT NUMBER(S)	
12. DISTRIBUTION/AVAILABILITY STATEMENT Approved for public release, distribution unlimited			
13. SUPPLEMENTARY NOTES See also ADM001736, Proceedings for the Army Science Conference (24th) Held on 29 November - 2 December 2005 in Orlando, Florida. , The original document contains color images.			
14. ABSTRACT			
15. SUBJECT TERMS			
16. SECURITY CLASSIFICATION OF:			17. LIMITATION OF ABSTRACT
a. REPORT unclassified	b. ABSTRACT unclassified	c. THIS PAGE unclassified	UU
			18. NUMBER OF PAGES 8
			19a. NAME OF RESPONSIBLE PERSON

FPA's of different formats. The objective of the test was to identify simulated combatants from non-combatants. This task is made relatively easy by the imagery from the 640×480 single-band FPA whereas the imagery from the 320×240 dual-band FPA was inconclusive at best. The imagery in Figure 1 shows that for unambiguous identification of targets, it is necessary to have many pixels on target.

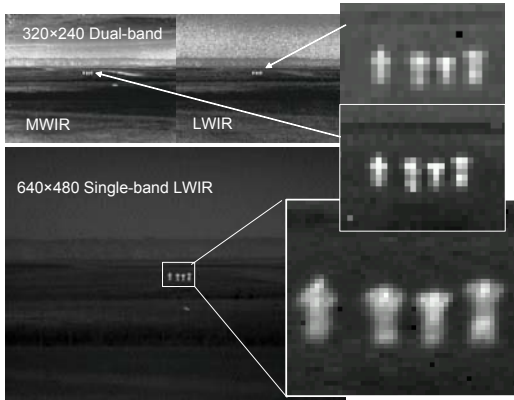


Figure 1. Imagery of people at a range of 500 m showing the advantage of high pixel count in identifying targets.

The pixel pitch for the 640×480 FPA that acquired the image in Figure 1 was 24 μm. This FPA was made by Lockheed Martin in 1998 using QWIPs. The size of semiconductor chips that may be fabricated easily using readily available processing equipment is limited to approximately 22 mm on a side. The limitation on the chip size in turn limits the size of the individual detectors to less than 20 μm for a 1024×1024 FPA. In this study a large format QWIP FPA produced using a conventional 2-dimensional grating optical coupler and the Santa Barbara Focalplane SBF-184 ROIC was tested in the lab and in the field.

Laboratory Tests

The large format QWIP FPA studied was produced by QWIP Technologies, Inc. of Altadena, CA (<http://www.qwip.com>) using bound-to-quasibound (BQB) detector structure and a 2-dimensional diffraction grating. The detector structure consisted of a stack of 50 quantum wells designed to have peak response near 8.5 μm. The detector array was hybridized to a the SBF-184 ROIC made by Santa Barbara Focalplane of Goleta, CA (a part of Lockheed Martin <http://www.sbf.com>). After hybridization the FPA was thinned using diamond-point turning to a final thickness of approximately 20 μm. The properties of the ROIC are shown in Table 1 below.

Table 1. Properties of the SBF-184 ROIC⁷

Property	Value
Format	1024×1024
Pixel size	19.5 μm square

Integration mode	Snapshot
Number of outputs	4, 8, or 16
Charge Well capacity	6.7E6 e ⁻ (0.43 pF)
Windowing	Yes – minimum window size = 512×8
Power dissipation	150 mW

The FPA was installed in a dewar/cooler assembly which used an AIM 2 Watt Stirling cycle cooler. The cooler was set to maintain a constant temperature such that the output voltage from a 2N2222 temperature sensor mounted on the ceramic package with the FPA was constant at 1.110 V (1 mA bias current). The temperature of the FPA could be changed through the use of an external 0 – 100 Ohm variable resistor placed in series with the internal temperature sensor. FPA temperatures between 60 K and 120 K could be set to a stability of ±0.02 K. The FPA was set up to run with 4 outputs active. In that configuration, the highest frame rate that could be achieved with our drive electronics was 16 Hz. The FPA was tested at operating temperatures ranging from 65 K to 95 K. Most of the measurements of FPA performance were done at 65 K.

Spectral Response

The results of the spectral response measurement are shown in Figure 2. The wavelength of maximum response was approximately 8.55 μm and the long wavelength cutoff (defined as the wavelength at which the response falls to half its maximum value) 8.7 μm while the short wavelength cutoff occurred at 8.0 μm. Due to limitations of the drive electronics hardware and software, the FPA was run in a format of 960 × 960 pixels.

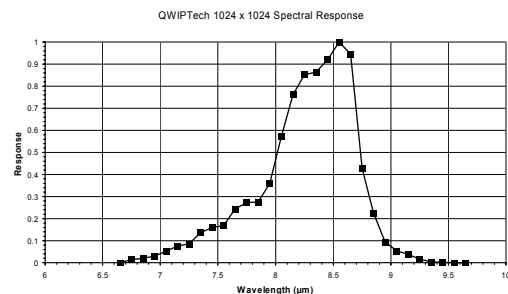


Figure 2. Spectral response of the QWIPTech large format FPA.

Current vs. Temperature

The total current (the sum of photocurrent and dark current) was measured at operating temperatures from 65 K to 95 K for several values of detector bias. The current was calculated from the known integration charge well capacity and the amount of integration

time needed to achieve saturation. Under those conditions, the current through the detector is given by

$$I = e(Q/\tau) \quad (1)$$

where e is the electronic charge, Q is the capacity of the charge well (6.7×10^6 electrons), and τ is the integration time. The results of the current measurements vs. bias and temperature are shown in Figure 3. For all values of bias used in this test, the current values at the three highest temperatures fall along a straight line when the log of the current is plotted against $1/kT$. The slope of this line which is the thermal activation energy for dark current was found to be 130 meV. The activation energy is expected to be slightly lower than the energy associated with a photon at the cutoff wavelength. At $8.7 \mu\text{m}$, the photon energy is 142 meV. The thermal activation energy calculated from the temperature dependence of the dark current is that which would be expected with detectors having the spectral characteristic shown in Figure 2.

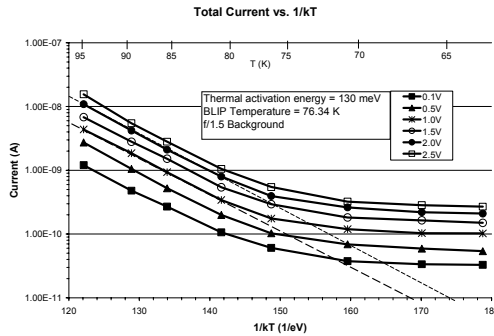


Figure 3. The temperature dependence of total current of the QWIPTech large format FPA showing that the background limited performance (BLIP) temperature is near 77 K.

Conversion Efficiency

Figure 4 shows the distribution of conversion efficiency (quantum efficiency – photoconductive gain product) across the QWIPTech FPA in the form of a pixel map and a histogram. The large size of this FPA (20 mm on each side, 28 mm diagonally) caused it to be difficult to illuminate the chip uniformly. The raw imagery showed a pronounced $\cos^4\theta$ roll-off of response toward the edges. The data shown in Figure 4 have been compensated for this effect in order to determine the true response uniformity of the FPA. The uncorrected non-uniformity is defined as the ratio of the standard deviation to the mean of the response distribution when no non-uniformity correction (NUC) applied. The FPA was rather uniform with an uncorrected non-uniformity of 12.3% over the entire array and an uncorrected non-uniformity of 3.5% in the central 256×256 sub-array. The number of inoperable pixels was just over 21,000 corresponding to 2.35% of the array. Most of the inoperable pixels were located

near the edges of the array and there were no large dead pixel clusters.

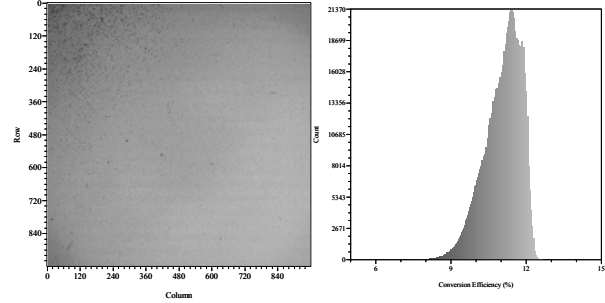


Figure 4. Conversion efficiency pixel map (a) and histogram (b) for the QWIPTech 1024×1024 FPA.

3D-Noise

The noise performance of the FPA was measured in terms of the NVESD 3-D Noise model.⁸ A two-point NUC was applied to the imagery with calibration temperatures of 24 °C and 32 °C provided by a calibrated extended-area blackbody source. Subsequently, two seconds of digital image sequences were collected at source temperatures between 18 °C and 38 °C. The data was analyzed using the 3D Noise module in Win-Proc software.⁹ The results of these calculations are shown in Figure 5. The temporal noise, tv_h , is relatively constant throughout the range of temperatures at a level just under 0.05 °C (50 mK). The other temporal components were very low which indicates that there was little or no overall image flicker or flashing of lines and/or columns. However, the random spatial fixed-pattern noise, vh , was quite high (comparable to or significantly higher than the temporal noise). The principal reason for the large value of fixed-pattern noise is the large variation in signal levels from the center to the edges of the chip. The dynamic range of the uncorrected pixel output is larger than the difference between the mean response to the hot and cold sources used for the NUC. This caused digitization errors in the code that calculated the gain and offset coefficients that were used in the NUC. These errors manifested themselves as concentric rings of different offset levels across the FPA. The problem is mitigated somewhat when the NUC is done for just a relatively small region (256×256) near the center of the FPA. An improved digital signal processor (DSP) board that is able to carry out the NUC calculations with more bits of precision will eliminate most of this problem.

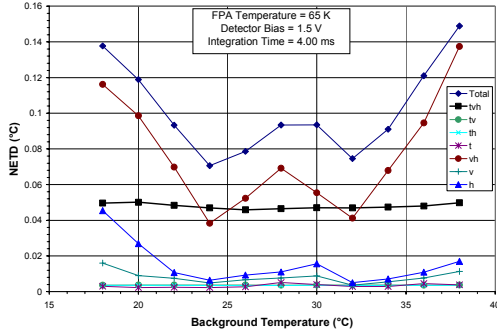


Figure 5. Results of 3-D noise measurements on the QWIP-Tech FPA.

We believe that electromagnetic interference (EMI) noise from the closed-cycle cooler generated a significant part of the noise that resulted in the measured values of the temporal NEAT shown in Figure 5. The white noise in the imagery was found to drop by nearly a factor of 2 when the cooler was shut off momentarily. Therefore, we estimate that the actual temporal NEAT of the FPA was on the order of 25 mK. We can calculate the temporal NEAT that would be expected for this FPA under BLIP conditions from the charge well capacity, the background temperature, T_B , and the photoconductive gain, g , using the expression

$$NE\Delta T = \frac{T_B}{2} \sqrt{\frac{g}{Q}} \text{ K} \quad (2)$$

if the charge well is half full.⁶ If the well is kept nearly full then the value of NEAT will be reduced by a factor of $\sqrt{2}$. The value of the photoconductive gain for the detectors in this FPA may be inferred from measurements of g on QWIPs of similar design. At bias levels around 1.5 V for a 50 well QWIP structure (electric field of 5 kV/cm), $g \approx 0.4$. Thus, given that the charge well capacity was 6.7 million electrons and a background temperature of 295 K, the temporal NEAT predicted by (2) would be 31.2 mK for a half-full charge well and 22.1 mK for a nearly full charge well. These values are consistent with the estimate of temporal NEAT with no cooler EMI given above.

Minimum Resolvable Temperature

Figure 6 shows the results of measurements of the minimum resolvable temperature (MRT) vs. spatial frequency of standard 4-bar targets. The bars of the targets were horizontal in all cases so this measurement is of the vertical MRT. Since the pixels of the FPA are square and there is no scanner, we expect there to be little difference between vertical and horizontal MRT. The bar targets ranged in frequency from 0.25 to 2.0 cycles/mrad. The pixels of the FPA were 19.5 μm on a side and the focal length of the lens was 100 mm so the

instantaneous field of view for each pixel was 0.195 mrad and the Nyquist spatial frequency was 2.56 cycles/mrad. Therefore, if there was no significant optical crosstalk, we expected to be able to resolve the highest frequency target. The MRT curve in Figure 6 follows the behavior expected of an imaging system with good modulation transfer function (MTF) and the highest spatial frequency target was resolved indeed. The low frequency MRT was 40 mK which is lower than the value of temporal NEAT. The MRT measurement is a subjective visual test in which the eye-cortex “signal processing” system is able to average many frames so that the experimenter can “see” the 4-bar pattern at levels of contrast below the value of NEAT.

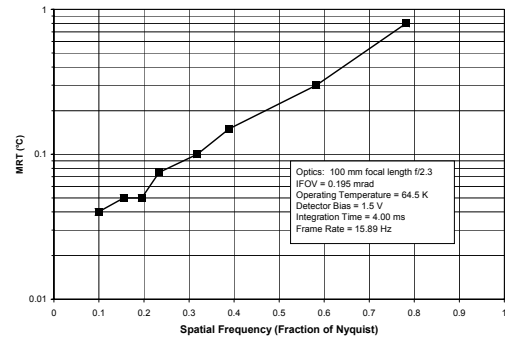


Figure 6. Vertical MRT vs. spatial frequency for QWIPTech 1024x1024 FPA.

Indoor Imagery and Optical Crosstalk

Figure 7 shows some example images acquired with the QWIPTech 1024x1024 FPA. The level of detail that can be resolved with this FPA cannot be appreciated in the full frame images. However, if one applies a digital zoom, these details become apparent. This FPA is capable of acquiring stunningly sharp IR images that could reveal details of targets that would be missed by smaller format FPAs. In Figure 7a the blackbody was set at 1000 K. The aperture was 0.375 mm (0.0125 in) wide. The aperture is clearly resolved in the digital zoom image with only a minimal amount of crosstalk considering the very high temperature of the source. The image of the lab and the person (Dr. K. K. Choi) shown in Figure 7b was acquired at an FPA temperature of 77.8 K. The integration time needed to be reduced from its value of 4.00 ms at 65 K to 2.62 ms but the image quality did not degrade significantly. The digital zoom image shows details of the test equipment (BNC connectors approximately 1 cm high) that were clearly resolved at a range of nearly 10 m.

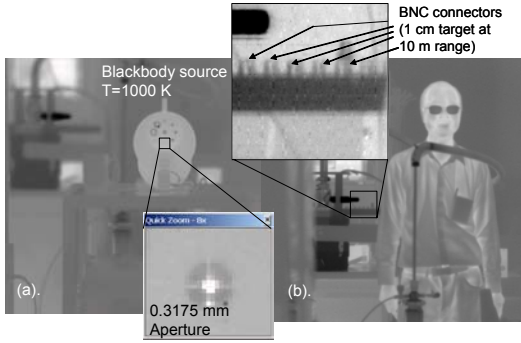


Figure 7. Example images acquired with the QWIPTech 10241024 FPA. The image of the person and the lab equipment was acquired at an FPA temperature of 77.8 K.

The magnitude of blooming was determined from images of a high-temperature (1000 K) blackbody source with small circular apertures ranging in size from 0.0125 in (0.3175 mm) to 0.4 in (10.16 mm) in diameter. Figure 8 shows 50×50 pixel section of images such as that in Figure 7b. The two smallest apertures were sub-pixel targets. The grey circles show the actual size of the larger targets. These images show that high flux sources can cause significant blooming in this FPA.

The crosstalk and blooming observed under the conditions described above are not generic to QWIPs. We have acquired similar imagery using a 640×480 QWIP FPA manufactured by BAE Systems and Lockheed Martin in 1998. In that case, the saturated region of the FPA is only slightly larger than the actual blackbody apertures for the largest targets. The principal difference between the two QWIP FPAs is that for the BAE Systems/Lockheed Martin FPA the GaAs substrate of the detector array was completely removed through a combination of mechanical polishing and reactive ion etching while that of the QWIP Technologies FPA was removed to a final thickness of less than 20 μm by diamond-point turning. The residual substrate thickness may be allowing light to be reflected back toward the active regions of neighboring detectors.

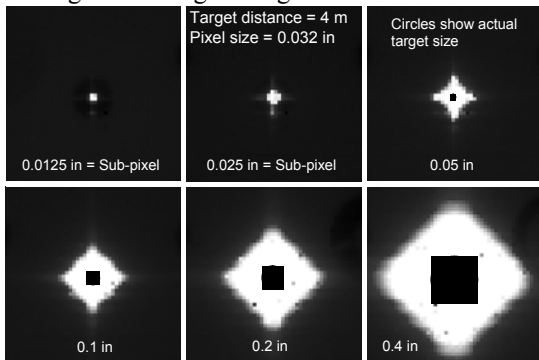


Figure 8. Images of a high-temperature (1000 K) blackbody acquired with the QWIP Technologies 1024×1024 FPA.

Figure 9 shows a schematic diagram of a small part of the QWIP with a 20 μm residual substrate (a) and with

a substrate that has been completely removed leaving less than 1 μm of material above and between the detector elements. If the substrate is thick compared with the thickness of the detector element (~ 5 μm) the incident light that is diffracted by the grating on each pixel can reflect off of the back surface of the FPA and induce signal at detectors that may be several pixel lengths away from the element location at which the light entered the FPA. This can lead to substantial blooming of a high-flux source. The crosstalk and blooming were found to be substantial only for high blackbody temperatures.

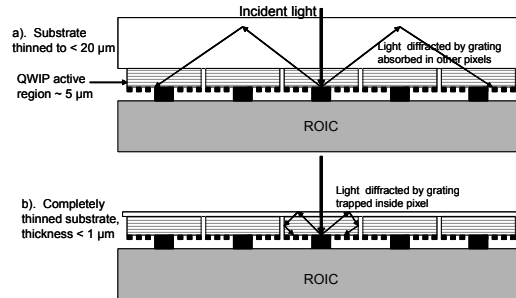


Figure 9. Schematic diagram comparing incomplete (a) and complete (b) substrate thinning.

Field Imagery

The camera system with the QWIP Technologies FPA installed was taken to a field test where various vehicles of military interest were viewed at ranges from 500 m to 5 km. The operational parameters of the camera are shown in Table 2. To calibrate the images in terms of source radiance, a cluster of 4 extended-area blackbodies were placed approximately 100 m from the camera. The blackbodies were imaged periodically throughout the test to determine calibration curves of response vs. radiance for the sensor. The calibration curves were quite linear with a correlation coefficient greater than 0.999. Examples of the imagery that was acquired during this test are shown in Figure 10. Even with a relatively short focal length and small aperture, the large number of pixels on target that were possible using this FPA made it relative easy to identify these targets at long ranges.

Table 2. Operational configuration of the large format QWIP camera in the field.

Parameter	Value
Operating Temperature	65 K
Detector Bias	2.0 V
Integration time	3.5 – 4.0 ms
Frame Rate	16 Hz
Optics focal length	100 mm
Pixel field of view	0.195 mrad
Total field of view	10.72°
Pixel size at 500 m, 1 km, and 5 km	9.75 cm, 19.5 cm, 97.5 cm

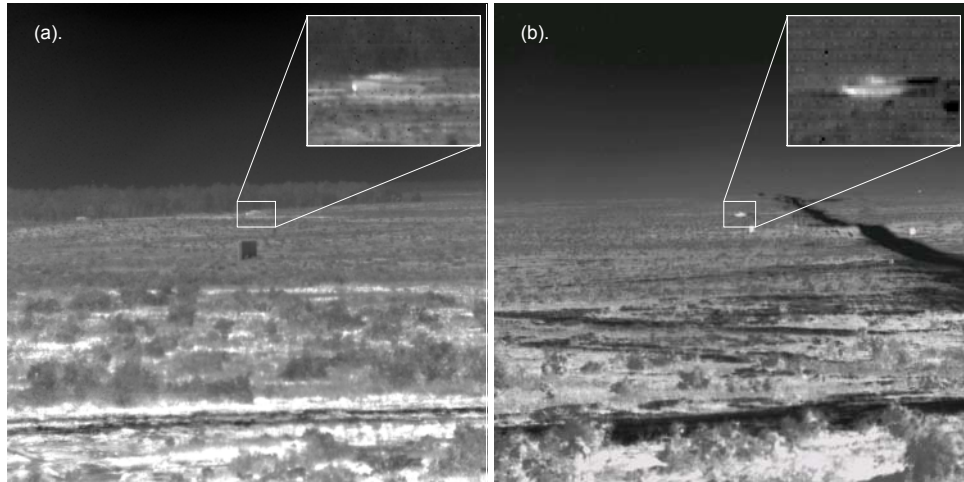


Figure 10. Image of an M1 tank at a range of 1 km (a) and a T72 tank at a range of 1.5 km (b). The insets show magnified the part of the images inside the white boxes.

The camera was taken to an observation platform overlooking a tributary of the Potomac River. Imagery was acquired of ground and airborne targets. Examples of these images are shown in Figure 11. In Figure 11(a) it is possible to detect the smokestack of a coal-fired electric power plant that was 30 km from the observation position; the upper inset shows a the part of the image containing the smokestack magnified. The lower inset shows a magnified image of the part of the master image containing the boat. Figure 11(b) shows an image of a Blackhawk helicopter at a range of approximately 7 km. A 64×64 pixel region surrounding the target is magnified in the inset image. Note the hot engine at the top of the target and that the integration time is short enough that the rotor blades are effectively “frozen.” In Figure 11(b) the sky background,

which usually presents a great challenge to LWIR FPAs, is imaged clearly and evenly and the details of the clouds are clearly seen as well.

Range Performance Modeling

Both the NVTherm (version: December 2002) and TRM-3 (version 2, July 2000) range models were used to predict the performance of the megapixel FPA camera in the configuration that was used in the field test. The models were set up for the relatively wide field of view of the 100 mm focal length lens (11.4° in horizontal and vertical directions). The model target approximated a T-72 tank (3 m high, 7 m long) under relatively benign atmospheric conditions. The scene contrast and the target contrast were both assumed to be 2 °C. The results obtained from the two range models are shown Table 3.

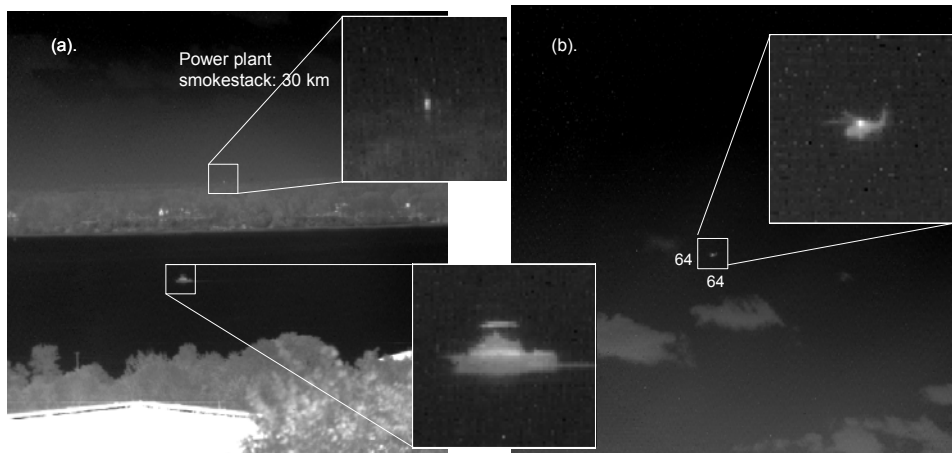


Figure 11. Images acquired of ground targets (a) and a Blackhawk helicopter (b) from a position overlooking part of a tributary of the Potomac River. The upper inset in (a) shows the detection of a power plant smokestack that was 30 km away. The lower inset in (a) shows a magnified image of the boat on the river. The inset in (b) is a magnified region of the image showing details of the helicopter.

Table 3. Results of range modeling of QWIPTech 1024×1024 FPA for a tank-sized target.

Probability	Number of resolved line pairs	NVTherm range (km) US Standard Atmosphere (1976)	TRM-3 range (km) Extinction = 0.2 km ⁻¹	TRM-3 range (km) Extinction = 1.0 km ⁻¹
50% Detection	0.75	> 10	12.21	4.55
90% Detection	1.8	8.50	7.61	3.84
50% Recognition	3.0	3,75	4.92	3.1
90% Recognition	5.4	2.10	2.86	2.31
50% Identification	6.0	1.90	2.59	2.14
90% Identification	10.5	1.10	1.50	1.34

The range performance predicted by both the TRM-3 and the NVTherm models for the QWIPTech FPA was about the same. Both models predict a 50% detection range for benign atmospheric conditions of more than 10 km. TRM-3 predicted a 36% longer range for a 50% probability of identification than NVTherm (2.59 km as opposed to 1.90 km). The range performance for the QWIP 1024×1024 FPA predicted by TRM-3 is shown in Figure 12 while that predicted by NVTherm is shown in Figure 13.

What is the reason for differences in predicted range performance between these models? More importantly, which of the models predicts the actual behavior of the sensor? We can get an insight into the answers to these questions by looking at the MRT vs. spatial frequency behavior predicted by both models and compare them to the measured data (shown in Figure 6).

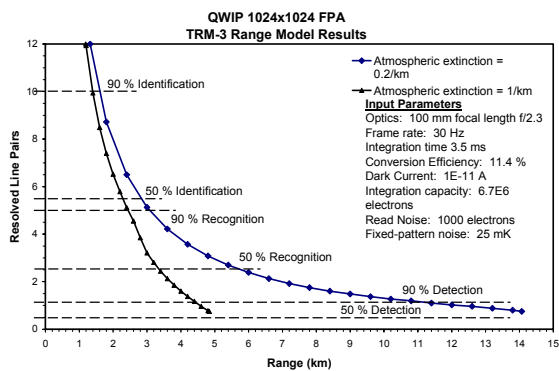


Figure 12. Range performance predicted by TRM-3 model for the QWIPTech 1024×1024 FPA with 100 mm focal length optics.

Figure 14 shows a comparison between the MRT values predicted by NVTherm and TRM-3 with those measured in the laboratory. Both models predict MRT values that are well below those measured in the laboratory over the full range of spatial frequencies. The TRM-3 model underestimates the MRT by about a factor of 6 over the entire range of spatial frequencies but the slope of the MRT vs. spatial frequency curve predicted by TRM-3 is about the same as that for the measured data. It is interesting that the MRT predicted

by NVTherm while lower than the measured data at low spatial frequencies, rises at a significantly higher rate than the measured values as the spatial frequency increases. This may explain why the recognition and identification ranges predicted by NVTherm are somewhat shorter than those predicted by TRM-3. Recognition and identification of targets require the resolution of high spatial frequencies. If, as NVTherm predicts, the MRT at high spatial frequencies is high then the range at which those high spatial frequencies can be resolved is relatively short given atmospheric extinction and other factors that tend to wash out the intrinsic thermal contrast of the target.

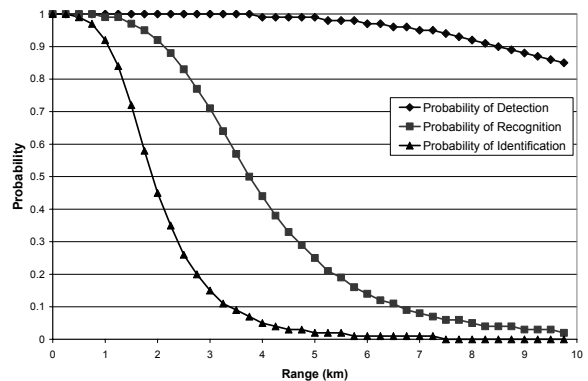


Figure 13. Probability vs. range for detection (diamonds), recognition (squares) and identification (triangles) predicted by the NVTherm model for the 1024×1024 QWIP FPA with 100 mm focal length optics.

The question still remains, which model more accurately predicts the range performance of this FPA/camera? Only a detailed analysis of imagery of targets in the field with accurate ground truth can settle this question. We have collected a substantial amount of this data in recent field tests. Presently the data is being analyzed and the results of this analysis will be reported in the near future.

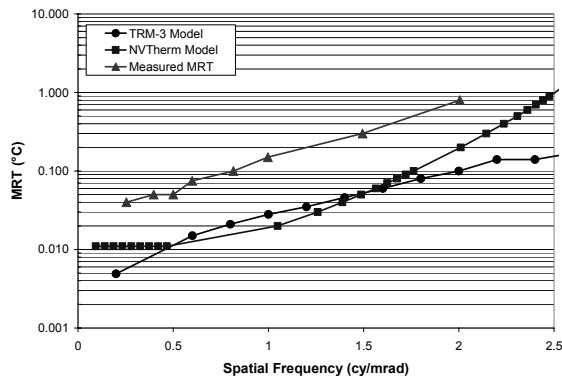


Figure 14. MRT vs. spatial frequency as predicted by NVTherm (squares) and TRM-3 (circles) models compared to measured data (triangles).

Conclusions

We have shown that QWIP detector technology can be applied to the various aspects of 3rd generation FLIR. First, very large format (1024×1024) focal plane arrays have been produced with excellent performance in terms of sensitivity, operability, and response uniformity. Near-BLIP performance has been achieved at an operating temperature near 77 K.

We have shown that the QWIPTech 1024×1024 FPA has collected high-quality imagery in the field. With the combination of large format and small pixels, we were able to detect and identify targets at long ranges. We have compared the range performance predicted for this camera by the NVTherm and TRM-3 models and found that both models predict similar range performance in detection, recognition, and identification ranges. The TRM-3 model predicted approximately 36% longer range for identification of a tank-sized target than that for NVTherm. However, neither model accurately predicted the MRT performance of the system as measured in the lab.

Getting both large array format and multispectral capability in a single FPA will be a challenge to QWIPs as it is a challenge for the HgCdTe detector technology. However, given the relative maturity of the growth and processing techniques for the III-V materials used in QWIPs and the existing commercial foundry infrastructure for these types of devices, it would appear that QWIPs could very well be the technology that produces 3rd generation FLIR sensors that not only meet the system performance needs of FCS but at an affordable cost.

ACKNOWLEDGEMENTS

We gratefully acknowledge the assistance of many people who made this study possible. Mark Stegall, Charlie Burgett and SE-IR, Inc. have provided not only the best FPA test equipment but have provided excellent customer service without which this and many other studies would have been impossible. We would also like to thank Devon Walsh of Lockheed Martin Santa Barbara Focalplane for providing information about the SBF-184 ROIC. NVTherm range performance modeling software was provided by Dr. Ronald Driggers of the Army Night Vision and Electronic Sensors Directorate and TRM-3 software was provided by Dr. Elke Eggermann of the Ministry of Defense of the Federal Republic of Germany.

REFERENCES

- ¹S. Smith, L. C. Chiu, S. Margalit, A. Yariv, and A. Y. Cho, *J. Vac. Sci. Technol. B* 1, 376 (1983).
- ²J. Caufield, *et al*, "Simultaneous Integrating Staring Two Color IRFPAs," *Proceedings of the 1997 IRIS Detector Specialty Group Meeting on Detectors*, ERIM, (1998).
- ³M. Sundaram, *et al*, "Advances in QWIP FPA (2-Color and 1-Color) Technology," *Proceedings of the 1998 IRIS Specialty Group Meeting on Detectors*, ERIM, (1999).
- ⁴D. Scribner, J. Schuler, P. Warren, M. Satyshur, M. Kruer, "Infrared Color Vision: Separating Objects from Backgrounds," *Proceedings of the SPIE - Infrared Detectors and Focal Plane Arrays V*, **3379**, (1998).
- ⁵H. Pollehn and J. Ahearn, "Multi-Domain Smart Sensors," *Proceedings of the SPIE, Infrared Technology and Applications XXV*, **3698**, Orlando, FL (1999).
- ⁶A. C. Goldberg, S. W. Kennerly, J. W. Little, H. K. Pollehn, T. A. Shafer, C. L. Mears, H. F. Schaake, M. Winn, M. Taylor, and P. N. Uppal, "Comparison of HgCdTe and QWIP Dual-Band Focal Plane Arrays", *Optical Engineering*, , Vol. **4369**, pp. 75-90 (2003).
- ⁷Santa Barbara Focalplane web site http://www.sbf.com/sbf_staring_fpa_family.htm.
- ⁸J. D'Augustino and C. Webb, "3-D Analysis Framework and Measurement Methodology for Imaging System Noise," in *Infrared Imaging Systems: Design, Analysis, Modeling and Testing II*, G. Holst, Editor, *Proceedings of the SPIE* Vol. 1488, 110-121, 1991.
- ⁹Developed by EOIR Technologies, <http://www.eoir.com/products/winproc.htm>